Cold-Crystallization Kinetics of Syndiotactic Polystyrene

Hongbin Lu, Steven Nutt

Department of Materials Science, University of Southern California, Los Angeles, California 90089

Received 22 April 2002; accepted 11 January 2003

ABSTRACT: The kinetics of the isothermal and nonisothermal cold crystallization of syndiotactic polystyrene (s-PS) were characterized with differential scanning calorimetry. A Johnson–Mehl–Avrami analysis of the isothermal experiments indicated that the cold crystallization of s-PS at a constant temperature followed a diffusion-controlled growth mode with a decreasing nucleation rate. Furthermore, the slow nucleation rate was the controlling step of the entire kinetic process. For nonisothermal cold-crystallization kinetics, we used a simple model based on a combination of the well-known Avrami and Ozawa models. The analysis revealed that, unlike for melt crystallization, the Avrami and Ozawa exponents were not equal. The activation energies for the isothermal and nonisothermal cold crystallizations of s-PS were 792.0 and 148.62 kJ mol^{-1}, respectively, indicating that the smaller motion units in cold crystallization had a weaker temperature dependence than those in melt crystallization. © 2003 Wiley Periodicals, Inc. J Appl Polym Sci 89: 3464–3470, 2003

Key words: syndiotactic; polystyrene; crystallization; differential scanning calorimetry (DSC); kinetics (polym.); growth

INTRODUCTION

The properties of semicrystalline polymers largely depend on the crystal structure and morphological evolution, the latter being closely related to external conditions such as the crystallization temperature.[1,2] Since the successful synthesis of syndiotactic polystyrene (s-PS) was reported in 1986,[3] s-PS has been used in a variety of applications in many fields and has been widely investigated. Early studies focused on the polymorphic behavior of s-PS.[4–10] These studies concluded that the polymorphic behavior of s-PS was complex, involving as many as four major crystal modifications (α, β, γ, and δ), depending on the thermal history and/or solution treatments. Recent studies[10–15] revealed that α and β modifications with a zigzag planar conformation could be obtained via melt crystallization, whereas γ and δ modifications with helical conformations were obtained by crystallization in the presence of solvents such as toluene.

The melt-crystallization kinetics for s-PS were reported recently. Work by Cimmino et al.[16] indicated that under isothermal conditions, the nucleation rate of s-PS was rapid, exceeding the nucleation rate of isotactic polystyrene (PS). However, the nonisothermal crystallization kinetics of s-PS were found to depend strongly on the sample molecular weight.[17] A comparison of the nucleation rate (i) and growth rate (g) in the melt crystallization of s-PS revealed different crystallization regimes:[18] in regime I, $i \ll g$; in regime II, $i \cong g$; and in regime III, $i > g$. The transition from regime II to regime III reportedly occurred at 512 K.[18] Analyses of isothermal and nonisothermal kinetics by the same authors led to the corresponding crystallization parameters for s-PS, such as the lateral and fold surface free energies, chain folding work, and activation energies.

The crystallization of amorphous polymers above the glass-transition temperature (T_g) is called cold crystallization. Unlike melt crystallization, in which the motion of polymer chains can be carried out entirely via molecular reptation,[19–21] the polymer chains in the rubber state complete the corresponding conformation rearrangement via cooperative segmental movements.[22] As a result, the crystal structure obtained from cold crystallization is expected to differ from structures obtained by melt crystallization. This was confirmed by Woo et al.,[11] who reported only one melting peak (α modification) for cold-crystallized s-PS, whereas three melting peaks, corresponding to α (peaks II and III) and β (peak I) modifications, were observed from melting differential scanning calorimetry (DSC) curves.

The molecular motion of semicrystalline polymers above T_g involves interactions between amorphous and crystalline regions.[23] The formation and development of crystalline regions inevitably limits the motion of polymer chains in the amorphous region. An investigation of the cold-crystallization behavior of amorphous samples would contribute to a further understanding of the kinetic behavior of polymer chains under confined conditions. The objective of this article is to characterize the cold-crystallization kinetics of

Correspondence to: S. Nutt (nutt@usc.edu).
Contract grant sponsor: TRW Foundation.

s-PS under isothermal and nonisothermal conditions with DSC.

EXPERIMENTAL

Material and sample preparation

Semicrystalline s-PS pellets were acquired from Scientific Polymer Products, Inc. (Ontario, NY). The syndiotacticity of s-PS was 90%, the density was 1.05×10^3 kg m^{-3}, and the melting temperature (T_m) and T_g were 270 and 100°C, respectively. The samples were prepared for cold-crystallization experiments according to the following procedure. The s-PS pellets were first placed between two microslides on a hot stage preset at 310°C. After being melted and pressed into flat disks about 0.5 mm thick, the samples were quenched in an ice–water bath, and this produced amorphous s-PS samples. Disks 4 mm in diameter were cut from the quenched samples and used for the DSC measurements.

DSC characterization

The cold-crystallization experiments of s-PS were performed with a differential scanning calorimeter (Thermal Analysis DSC 2920) under an atmosphere of N_2 (flow rate = 60 mL/min). The apparatus was calibrated with indium and zinc standards (T_m = 156.6 and 419.5°C) at a heating rate of 10°C/min. In isothermal experiments, the samples were heated rapidly to 127, 128, 129, 130, and 131°C and held at the corresponding temperatures for the desired time. The heat flow was recorded at 2-s intervals. Nonisothermal experiments were conducted under a nitrogen atmosphere at heating rates of 5, 10, 20, 30, 40, and 50°C/min. Baseline data obtained from the empty sample pan were subtracted from all data files.

RESULTS AND DISCUSSION

Isothermal crystallization kinetics

Isothermal cold-crystallization experiments were performed at temperatures about 30°C above T_g of s-PS so that the transformation of s-PS from the amorphous state to the crystalline state could be resolved clearly. The experimental results at different temperatures are presented in Figure 1(a). The cold-crystallization rate markedly increases with increasing temperature, despite a temperature interval of only 1°C. Figure 1(b) shows the corresponding relative degree of crystallinity [$X_t = \int_1^\infty (dH/dt)dt / \int_0^\infty (dH/dt)dt$] as a function of time t at various crystallization temperatures. The strong dependence of the cold-crystallization rate on the temperature is evident.

The temperature dependence of the cold-crystallization rate for s-PS is similar to the melt-crystallization

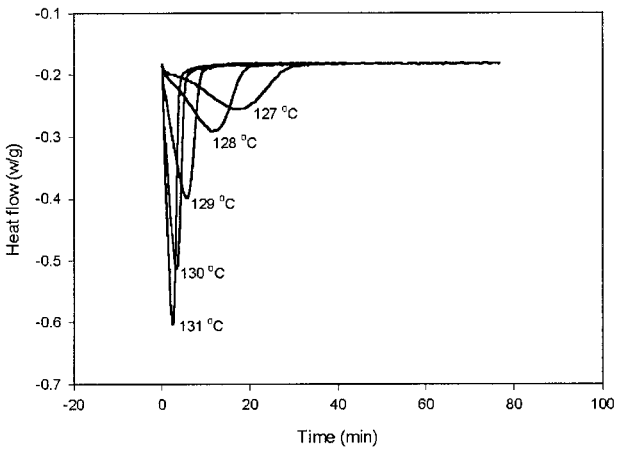

(a)

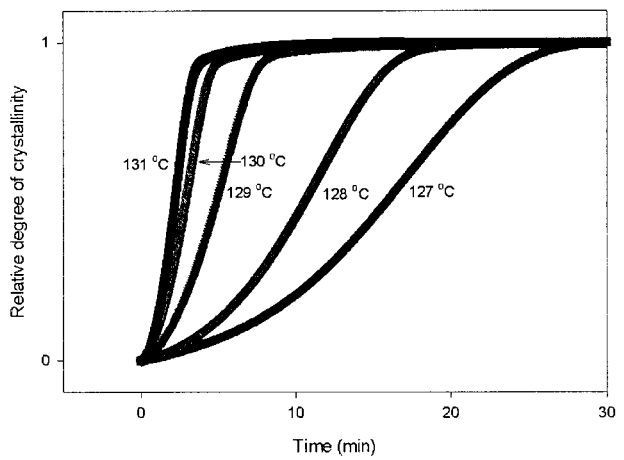

(b)

Figure 1 (a) Original DSC curves for isothermal cold crystallization of s-PS and (b) relative degree of crystallinity with time at different crystallization temperatures.

kinetics of s-PS,[18] often described by the Johnson–Mehl–Avrami (JMA) equation.[24,25] The JMA equation is based on the theory of transformations governed by nucleation and growth kinetics. In fact, the JMA equation is widely used to describe time-transformation isotherms of many solid-state processes.[26–28] A comprehensive review, including the derivation and applications of the JMA equation, was given by Christian.[29] The JMA equation can be simply written as follows:

$$\log[-\ln(1 - X_t)] = \log k + n \log t \qquad (1)$$

where k is the overall kinetic rate constant, t is the isothermal crystallization time, n is the Avrami expo-

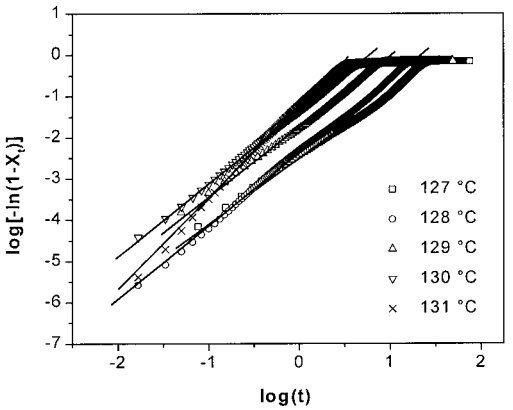

Figure 2 JMA plot of isothermal cold-crystallization data for s-PS at selected temperatures.

nent, and X_t is the relative crystallization fraction at t. The values of k and n are obtained by plotting of the left-hand side of eq. (1) versus log t, as shown in Figure 2. The plot shows the linear behavior of the crystallization rate for s-PS samples at different crystallization temperatures, and the corresponding parameters extracted from Figures 1(b) and 2 are listed in Table I. Unlike melt crystallization, which is driven by undercooling,[19] the cold crystallization of polymers often requires a certain amount of energy to overcome the potential barrier to molecular segmental motion. Therefore, cold-crystallization rates generally increase with temperature, and this is consistent with the rate constants in Table I. Note that these rate constants for the cold crystallization of s-PS are more than 2 orders of magnitude lower than those for melt crystallization.[18] Such low crystallization rates primarily stem from the constraint of crystalline regions to amorphous molecular mobility.

When the JMA equation is used to describe the kinetic behavior of crystallization, discrepancies between the experimental data and theory are often observed. This is especially true in the latter stages of crystallization,[30] as shown in Figure 2. Moreover, deviations appear earlier with decreases in the cold-crystallization temperature (T_c). The deviations result from two factors: (1) the impingement of spherulites and (2) the constraint of molecular mobility arising from the expansion of crystalline regions and/or increased entanglements. These factors alter the cold-crystallization behavior in the latter stages and render a theoretical description more difficult.

Nevertheless, in the absence of a more suitable model, the JMA equation can be used to predict the salient features of cold-crystallization kinetics.[1] As shown in Figure 2, two distinct stages are manifest during isothermal crystallization. Fitting the experimental data from the early stage yields n values in the range of 1.6–2.2 (Table I). These values suggest a diffusion-controlled growth mode accompanied by a decreasing nucleation rate. This means that in the cold crystallization of s-PS, the constraint of crystalline regions not only hinders the growth of spherulites but also reduces the nucleation rate and eventually leads to a decrease in the overall crystallization rate. Similar behavior was reported by Ivanov et al.,[23] who studied the isothermal cold crystallization of poly(ether ether ketone) (PEEK) with small-angle X-ray scattering and dynamic mechanical analysis. They concluded that at least two crystallization mechanisms could be acting during the isothermal cold crystallization of PEEK. The early behavior was related to conventional nucleation, growth, and impingement of spherulites. However, in the second stage, free amorphous regions disappeared, and more complex kinetics governed the crystallization behavior of the system.

As mentioned previously, the motion unit in melt crystallization may be chain segments or the entire chain, whereas the motion unit in cold crystallization is just a segment of the macromolecule. Therefore, the temperature dependence of the two crystallization processes can differ, and this phenomenon should be reflected in different activation energies. For thermally activated processes such as cold crystallization, the activation energy can be obtained from an Arrhenius relationship:

$$\frac{1}{n}\ln k = \ln K_0 - \frac{\Delta E_i}{RT_c} \tag{2}$$

where k is the cold-crystallization rate constant, K_0 is the temperature-independent pre-exponential factor, R is the universal gas constant, and ΔE_i is a total activation energy for crystallization processes. This activation energy can be determined by the plotting of the left-hand side of eq. (2) versus the reciprocal of T_c (Fig. 3). As expected, the value of ΔE_i obtained from Figure 3 (792.0 kJ mol^{-1}) is lower than the activation energy for melt crystallization reported by Chen et al.[18] (830.7 kJ mol^{-1}). The crystallization in the melt involves the reptation of entire polymer chains, which requires more energy to achieve conformational rearrangement. The crystal structure formed during cold crystallization is likely to be less perfect, and the material will exhibit a lower T_m than the melt-crystallized polymer. Such differences in crystal structure during

TABLE I
Kinetic Parameters Obtained from Isothermal Cold-Crystallization Experiments and Avrami Analysis

T_c (°C)	n	k (min^{-n})	$t_{1/2}$ (min)
127	1.6	0.00309	16.02
128	1.8	0.0042	10.67
129	1.7	0.0181	5.04
130	1.8	0.04256	2.94
131	2.2	0.0561	2.18

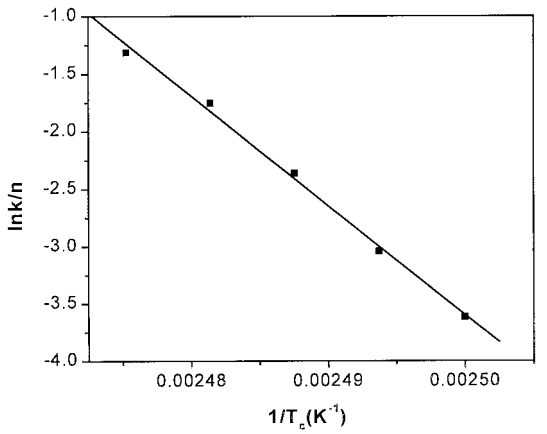

Figure 3 Dependence of the isothermal cold-crystallization rate constant ($\ln k/n$) on the temperature ($1/T_c$).

cold and melt crystallizations were confirmed by Woo et al.[11] In their work, the high-temperature melting peak for melt crystallization was about 3°C higher than the melting peak for cold crystallization.

To further explore the cold-crystallization kinetics of s-PS, we can determine the nucleation rate parameter on the basis of the secondary nucleation theory developed by Hoffman and Miller.[19] This theory was used by Qiu et al.[31] to analyze the cold-crystallization kinetics of poly(aryl ether ketone ether ketone ketone). When the crystal growth rate equation of Hoffman and Miller is combined with the JMA equation describing the overall crystallization kinetics, the overall crystallization rate can be expressed by a generalized equation:

$$\frac{1}{n}\ln k(T) + \frac{U^*}{R(T_c - T_0)} = A_n - \frac{K_g\,(T_c + T_m^0)}{2T_c^2\,(\Delta T)} \qquad (3)$$

where $k(T)$ and n are the parameters in the JMA equation, U^* is the transport activation energy that governs the short-distance diffusion of the crystalline unit across the phase boundary and has a universal value of 1500 kcal mol^{-1}, T_0 is the temperature below which segmental motion ceases ($T_0 = T_g - 30$), T_m^0 is the equilibrium melting temperature, ΔT is the degree of supercooling and is equal to $T_m^0 - T_c$, K_g is the nucleation rate constant, and A_n is a constant.[19] A plot of the left-hand side of eq. (3) versus $(T_c + T_m^0)/2T_c^2(\Delta T)$ will produce a line with slope K_g. Figure 4 displays such a plot, yielding K_g for an s-PS cold crystallization of 8.17×10^6 K^2.

In general, K_g can be written as follows:[19]

$$K_g = \frac{jb_0\sigma\sigma_e T_m^0}{k(\Delta h_f)} \qquad (4)$$

where b_0 is the monomolecular layer thickness, σ is the lateral surface free energy, σ_e is the fold surface free energy, k is Boltzmann's constant, and Δh is the enthalpy of fusion. The crystallization of polymers proceeds in three regimes.[19] In regime I, the crystal growth rate G varies with the surface nucleation rate i ($G \propto i$). With an increase in the nucleation rate (regime II), multiple nucleation occurs on the substrate ($G \propto i^{1/2}$). In a high-rate nucleating stage (regime III), the mean separation of nuclei on the substrate approaches the width of molecular stems (again, $G \propto i$). To determine which regime describes the cold crystallization at selected temperatures, we can use the Lauritzen Z test:[32]

$$Z \cong 10^3(L/2a_o)^2 \exp[-X/T_c(\Delta T)] \qquad (5)$$

where L is the effective lamellar thickness and a_0 is the chain stem width. Regime I kinetics are followed if the substitution of $X = K_g$ into eq. (5) results in $Z \leq 0.01$. If $X = 2K_g$, eq. (5) yields $Z \geq 1$, and regime II kinetics are followed. For s-PS, L is 18 nm,[33,34] a_0 is 0.441 nm, and T_m^0 is 286.6°C.[16,35] Therefore, the cold crystallization is clearly regime I. Consequently, for the cold crystallization of s-PS in a selected temperature range (127–131°C), the nucleation rate is slow, and nucleation constitutes the controlling step of the entire kinetic process.

Nonisothermal crystallization kinetics

The nonisothermal experimental crystallization behavior is presented in Figure 5(a,b), which shows the heat flow and crystallinity at different heating rates. As the heating rate is increased, the exothermic peak temperatures (T_p's) shift to higher temperatures and become broader. The trend is similar to that for the nonisothermal cold-crystallization behavior reported for other polymers, such as poly(aryl ether ketone

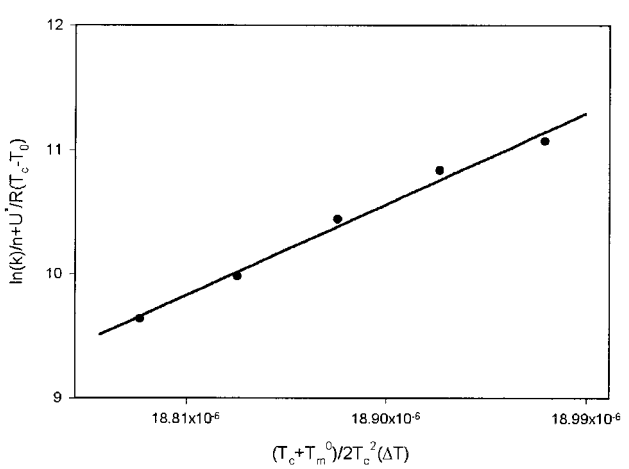

Figure 4 Determination of the nucleation rate constant by the combination of the Avrami equation and the secondary nucleation theory.

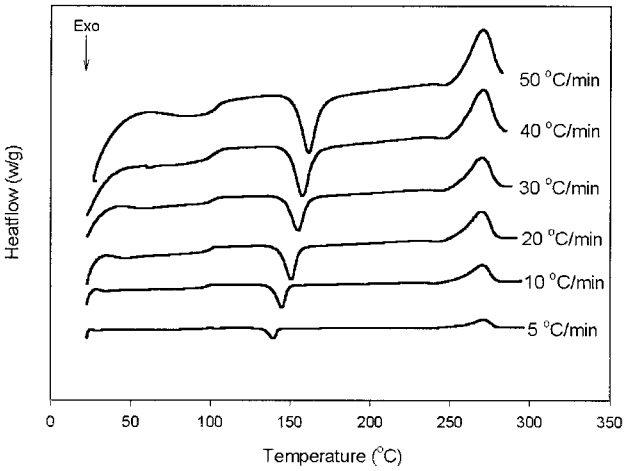

(a)

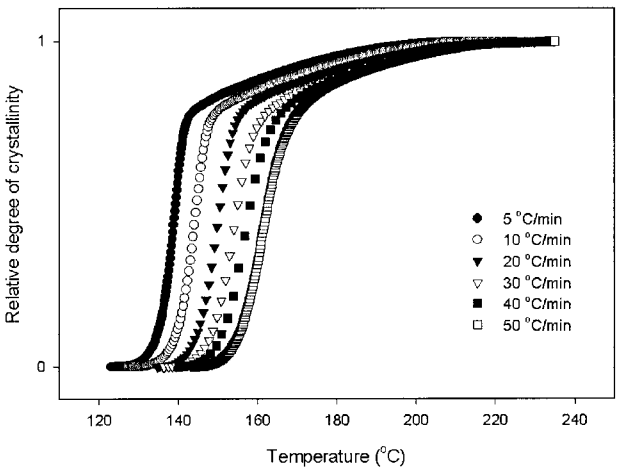

(b)

Figure 5 (a) Original DSC curves for nonisothermal cold crystallization of s-PS and (b) relative degree of crystallinity with temperature at various heating rates.

ether ketone ketone) (PEKEKK),[36] poly(aryl ether diphenyl ether ketone) (PEDEK),[37] and poly(aryl ether ether ketone ketone) (PEEKK).[38] The values of T_p and the exothermic enthalpy, ΔH, during the nonisothermal cold crystallization are given in Table II. The average value of ΔH is 20.09 kJ mol^{-1}, which is lower than the enthalpy of melt crystallization reported by

TABLE II
Peak Temperature and Enthalpy of s-PS Under Nonisothermal Cold-Crystallization Conditions

Heating rate (°C/min)	5	10	20	30	40	50
T_p (°C)	139.3	144.7	150.5	155.0	158.0	161.4
ΔH (J/g)	19.37	20.12	20.80	20.78	18.38	21.08

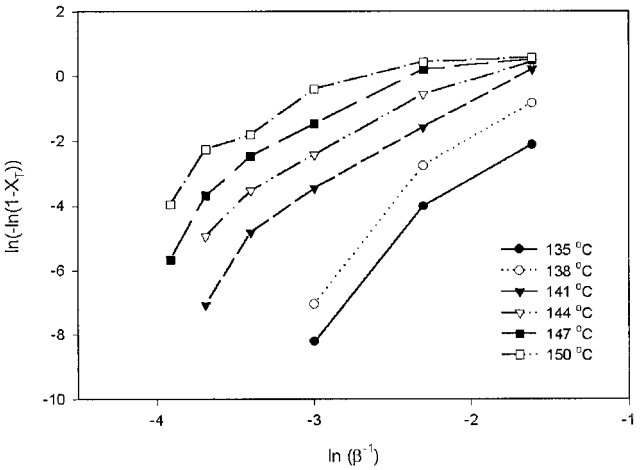

Figure 6 Ozawa plot of the nonisothermal cold crystallization of s-PS at various temperatures.

Chen et al.[18] (27.34 kJ mol^{-1}). The difference in the ΔH values can be attributed to the different syndiotacticities of the two sample materials. The syndiotacticity of s-PS studied by Chen et al. was 97%; the syndiotacticity was 90% for s-PS in this work.

To analyze the melt-crystallization kinetics of polymers, Ozawa[39] extended the JMA equation for isothermal crystallization to the nonisothermal case, assuming that the ambient temperature changed at a constant rate and employing the mathematical derivation of Evans.[40] In Ozawa's analysis, the transformation fraction during crystallization can be expressed as follows:

$$X_T = 1 - \exp\left[-\frac{K(T)}{|\beta|^m} \right] \tag{6}$$

where X_T is the transformation fraction, $K(T)$ is a nonisothermal crystallization rate constant, m is the Ozawa exponent, and β is the heating or cooling rate. Taking double logarithms of both sides of eq. (6) at a constant temperature and plotting them, we would expect to determine the values of m and $ln\ K(T)$ from the slope and intercept of a series of lines. However, as shown in Figure 6, the Ozawa plot does not yield a straight line for the experimental conditions used here. The absence of linearity indicates that the Ozawa equation does not accurately describe the cold-crystallization behavior of s-PS under nonisothermal conditions. The discrepancy can be attributed to the assumptions used in deriving the Ozawa model, such as the dependence of the lamellar thickness on the temperature and secondary crystallization.

An alternative model was recently proposed by Mo et al.,[38] who combined the JMA theory with the Ozawa equation to analyze the nonisothermal kinetics of several polymer systems, including cold crystalli-

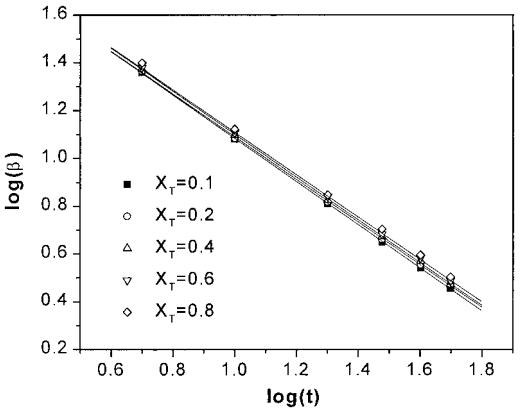

Figure 7 Application of a simple model proposed by Mo et al.[38] to the nonisothermal experimental data of s-PS for various values of the relative degree of crystallinity.

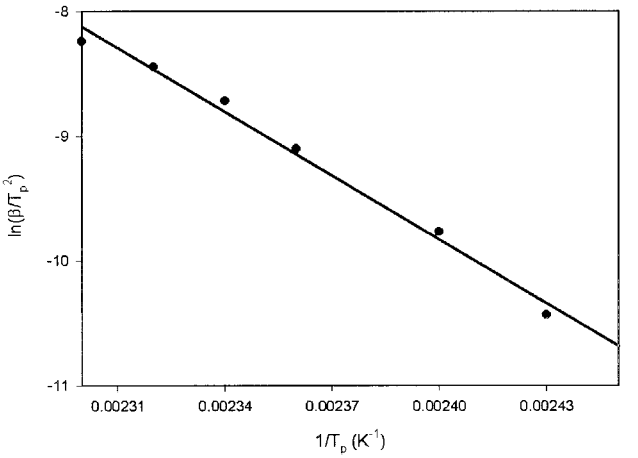

Figure 8 Determination of the activation energy for the nonisothermal cold crystallization of s-PS with the Kissinger method.

zation. The final expression of their model can be written as follows:

$$\log(\beta) = \log F(T) - a \log t \tag{7}$$

where the parameter $F(T)$ is a constant chosen at a unit crystallization time corresponding to a specified degree of crystallinity and a is the ratio of n to m ($a = n/m$). Plotting $\log \beta$ versus $\log t$ at different heating rates yields a series of lines, from which the values of $F(T)$ and a are obtained. Figure 7 shows these linear relationships, and the kinetic parameters obtained are listed in Table III. Unlike melt crystallization,[18] n is not equal to m, and $F(T)$ for cold crystallization is also much greater than for melt crystallization.

The activation energy for nonisothermal cold crystallization of s-PS can be obtained from the Kissinger equation:[41,42]

$$\frac{d \ln(\beta/T_p^2)}{d(1/T_p)} = -\frac{\Delta E_n}{R} \tag{8}$$

where T_p refers to the peak temperature of nonisothermal cold-crystallization curves and ΔE_n is the activation energy corresponding to nonisothermal cold crystallization. The Kissinger plot, shown in Figure 8, yields an activation energy of 148.62 kJ mol^{-1}. This value is smaller than the value obtained by Chen et al.[18] for melt crystallization (315.9 kJ mol^{-1}), indicating that the smaller motion units have a weaker temperature dependence in nonisothermal cold crystallization than in melt crystallization.

TABLE III
The Kinetic Parameters Obtained from the Model Proposed by Mo et al.[37]

	Relative degree of crystallinity				
Parameter	0.1	0.2	0.4	0.6	0.8
$F(T)$	1.99	1.98	1.99	1.99	1.99
a	0.90	0.89	0.90	0.89	0.90

CONCLUSIONS

The experimental results and analyses of the crystallization behavior of s-PS under isothermal and nonisothermal conditions has led to the following conclusions:

1. The isothermal cold crystallization of s-PS is a complex kinetic process for which only the early stages of crystallization are adequately described by the JMA model. The n value (1.5–2.2) indicates that isothermal cold crystallization may be followed by a diffusion-controlled growth mode accompanied by a decreasing nucleation rate. The activation energy is lower than the reported values for melt crystallization, implying a weaker temperature dependence for cold crystallization than for melt-crystallization processes. The results of the Lauritzen Z test indicate that during the isothermal cold crystallization of s-PS, nucleation is the rate-limiting step of the kinetic process.
2. The nonisothermal cold crystallization of s-PS can be described with a simple model proposed by Mo et al.[38] The kinetic parameters obtained from this model indicate that n is not equal to m during cold crystallization, contrary to the results for melt crystallization reported in the literature. The activation energy obtained by the Kissinger method, 148.62 kJ mol^{-1}, is also lower than the reported activation energy for nonisothermal melt crystallization, 315.9 kJ mol^{-1}.

3. On the basis of the experimental and theoretical analyses, this study on cold-crystallization kinetics provides a picture describing the transformation of s-PS molecules from the unordered state to the ordered state, especially in the early stage of cold crystallization. The constraint exerted by crystalline regions on molecules in amorphous regions leads to the breakdown of the JMA model in the latter stage. This behavior highlights a limitation of the JMA model in describing the cold-crystallization kinetics of polymers. These results indicate the need for a more refined theoretical treatment for the cold-crystallization kinetics of polymers that incorporates the effects of constrained motion of amorphous molecules.

The authors thank Hongbin Shen for his assistance with the DSC experiments and interpretation.

References

1. Wunderlich, B. Macromolecular Physics; Academic: London, 1976; Vol 2.
2. Long, Y.; Shanks, R. A.; Stachurski, Z. H. Prog Polym Sci 1995, 20, 651.
3. Ishihara, N.; Seimiya, T.; Kuramoto, M.; Uoi, M. Macromolecules 1986, 19, 2464.
4. Immirzi, A.; De Candia, F.; Iannelli, P.; Vittoria, V.; Zambelli, A. Makromol Chem Rapid Commun 1988, 9, 761.
5. Kobayashi, M.; Nakaki, T.; Ishihara, N. Macromolecules 1989, 22, 4377.
6. Guerra, G.; Vitagliano, V. M.; De Rosa, C.; Petraccone, V.; Corradini, P. Macromolecules 1990, 23, 1539.
7. Greis, O.; Xu, Y.; Asano, T.; Peterman, J. Polymer 1989, 30, 590.
8. Sun, Z.; Morgan, R. J.; Lewis, D. N. Polymer 1992, 33, 661.
9. De Rosa, C.; Rapacciuolo, M.; Guerra, G.; Petraccone, V.; Corradini, P. Polymer 1992, 33, 1423.
10. Chatani, Y.; Shimane, Y.; Ijitsu, T.; Yukinari, T. Polymer 1993, 34, 1625.
11. Woo, E. M.; Sun, Y. S.; Lee, M. L. Polym Commun 1999, 40, 4425.
12. Woo, E. M.; Wu, F. S. Macromol Chem Phys 1998, 199, 2041.
13. Sun, Y. S.; Woo, E. M. Macromolecules 1999, 32, 7836.
14. Tashiro, K.; Yoshioka, A. Macromolecules 2002, 35, 410.
15. Hodge, K.; Prodpran, T.; Shenogina, N. B.; Nazarenko, S. J Appl Polym Sci 2002, 83, 2705.
16. Cimmino, S.; Pace, E. D.; Martuscelli, E.; Corradini, P. Polymer 1991, 32, 1080.
17. Wesson, R. D. Polym Eng Sci 1994, 34, 1157.
18. Chen, Q.; Yu, Y.; Na, T.; Zhang, H.; Mo, Z. J Appl Polym Sci 2002, 83, 2528.
19. Hoffman, J. D.; Miller, R. L. Polymer 1997, 38, 3151.
20. Graessley, W. W. J Polym Sci Polym Phys Ed 1980, 18, 27.
21. Doi, M.; Edwards, S. F. J Chem Soc Faraday Trans 1978, 2, 1802.
22. Ferry, J. D. Viscoelastic Property of Polymers, 2nd ed.; Wiley: New York, 1970.
23. Ivanov, D. A.; Legras, R.; Jonas, A. M. Macromolecules 1999, 32, 1582.
24. Johnson, W. A.; Mehl, R. F. Trans Am Inst Miner (Metall) Eng 1939, 135, 416.
25. (a) Avrami, M. J Phys Chem 1939, 7, 1103; (b) Avrami, M. J Phys Chem 1940, 8, 212; (c) Avrami, M. J Phys Chem 1941, 9, 177.
26. Pradell, T.; Crespo, D.; Clavaguera, N.; Clavaguera-Mora, M. T. J Phys: Condens Matter 1998, 10, 3833.
27. Malek, J.; Mitsuhashi, T. J Am Ceram Soc 2000, 83, 2103.
28. Malek, J. Thermochim Acta 1995, 267, 61.
29. Christian, J. W. The Theory of Transformation in Metals and Alloys, 2nd ed.; Pergamon: New York, 1975.
30. Ruitenberg, G.; Woldt, E.; Petford-Long, A. K. Thermochim Acta 2001, 378, 97.
31. Qiu, Z.; Mo, Z.; Zhang, H.; Sheng, S.; Song, C. J Polym Sci Part B: Polym Phys 2000, 38, 1992.
32. Lauritzen, J. I. J Appl Phys 1973, 44, 4353.
33. Barnes, J. D.; McKenna, G. B.; Landes, B. G.; Bubeck, R. A.; Bank, D. Polym Eng Sci 1997, 37, 1480.
34. Lopez, L. C.; Cieslinski, R. C.; Putzig, C. L.; Wesson, R. D. Polymer 1995, 36, 2331.
35. Woo, E. M.; Wu, F. S. Macromol Chem Phys 1998, 199, 2041.
36. Qiu, Z.; Mo, Z.; Zhang, H.; Sheng, S.; Song, C. J Appl Polym Sci 2000, 77, 2865.
37. Qiu, Z.; Zhou, H.; Mo, Z.; Zhang, H.; Wu, Z. Polym J 2000, 32, 287.
38. Liu, T.; Mo, Z.; Wang, S.; Zhang, H. Polym Eng Sci 1997, 37, 568.
39. Ozawa, T. Polymer 1971, 12, 150.
40. Evans, U. R. Trans Faraday Soc 1945, 41, 365.
41. Henderson, D. W. J Non-Cryst Solids 1979, 30, 301.
42. Kissinger, H. E. Anal Chem 1957, 29, 31.